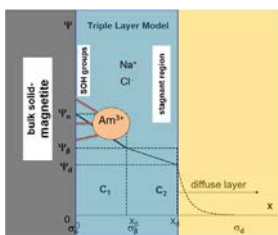


Sorption of americium / europium onto magnetite under saline conditions: Batch experiments, surface complexation modelling and X-ray absorption spectroscopy study

Nikoleta Morelová*, Nicolas Finck, Johannes Lützenkirchen, Dieter Schild, Kathy Dardenne, Horst Geckeis

Institute for Nuclear Waste Disposal (INE), Karlsruhe Institute of Technology (KIT), P.O. 3640, D-76021 Karlsruhe, Germany

GRAPHICAL ABSTRACT



ARTICLE INFO

Keywords:
Trivalent radionuclides
Sorption
Magnetite
XAS
Molecular mechanism
Complexation constants
Saline systems
CD-MUSIC model
Titration

ABSTRACT

Hypothesis: This study investigates the adsorption of americium and its chemical analogue europium on magnetite, which is expected to form as a major long term steel canister corrosion product under anoxic and highly saline conditions.

Experiments: The sorption of europium on magnetite (solid/liquid ratio = 0.5 g/L) was investigated batch wise in NaCl brines with ionic strength $I = 1\text{ m}$, 3.5 m , and 6.67 m , as a function of pH_m for two europium concentrations ($6 \times 10^{-10}\text{ m}$, $1.2 \times 10^{-5}\text{ m}$). Information on the chemical nature of the surface species was obtained by X ray absorption spectroscopy (XAS) at the americium L_3 edge.

Findings: Retention of europium by magnetite of $>99.5\%$ was found above pH_m 6.4 for all ionic strengths for europium concentration of $6 \times 10^{-10}\text{ m}$. No ionic strength effect was observed in this pH_m range. At $1.2 \times 10^{-5}\text{ m}$ europium concentration, $95 \pm 4\%$ sorption was found above pH_m 7.5 for $I = 1\text{ m}$ and above pH_m 8.0 for $I = 3.5\text{ m}$ and 6.67 m . A small ionic strength effect was observed in this case. X ray absorption spectroscopy (XAS) results are consistent with the batch sorption experiment outcomes, showing an insignificant effect of ionic strength on the pH_m dependent sorption. Results from potentiometric titrations of the solid phase, batch sorption experiments and spectroscopy were interpreted consistently with a charge distribution multi site (CD MUSIC) triple layer surface complexation model assuming surface coordination of the metal ion via a tridentate binding mode.

1. Introduction

Deep geological repositories have been selected as the most appropriate option for final disposal of high level radioactive waste. High level radioactive waste is expected to be emplaced inside various types of metallic containers, most of them made of steel [3]. One of the main corrosion products will be magnetite,

* Corresponding author.

E-mail addresses: nikoleta.morelova@kit.edu (N. Morelová), nicolas.finck@kit.edu (N. Finck), johannes.luetzenkirchen@kit.edu (J. Lützenkirchen), dieter.schild@kit.edu (D. Schild), kathy.dardenne@kit.edu (K. Dardenne), horst.geckeis@kit.edu (H. Geckeis).

as a stable crystalline iron corrosion product in moderately to strongly reducing environments and under neutral to alkaline conditions. Magnetite can be formed either by the Schikorr reaction at elevated temperature starting from $\text{Fe}(\text{OH})_2$ or by transformations of metastable phases such as layered double hydroxides (green rusts) [8]. Magnetite (Fe_3O_4) is a mineral with inverse spinel structure where tetrahedral positions are filled with only Fe(III), while the octahedral positions contain equal amounts of Fe(II) and Fe(III). Alternating planes of Fe_{tet} and Fe_{oct} are stacked along the (1 1 1) plane in the magnetite structure [48]. Furthermore, various experimental corrosion tests have confirmed the formation of magnetite under conditions relevant to deep geological repository environments [47,24,48]. Thus, the interaction of magnetite with radionuclides (RN) should be evaluated to allow prediction of their migration behaviour. The affinity of different actinides towards magnetite has been previously reported. U(VI) sorption on magnetite under anoxic conditions was studied by Missana et al. [32], and the interaction of U(VI) with magnetite generated in situ by corrosion was reported by Rovira et al. [42]. Further, the reducing effect of magnetite on U(VI) was investigated by Grambow et al. [15], Scott et al. [44], Ilton et al. [22], Huber et al. [21], Yuan et al. [50], Latta et al. [27] and Pidchenko [36]. Sorption and reduction of Np(V) was investigated by Nakata et al. [33], while Th(IV) sorption onto magnetite was reported by Rojo et al. [40]. Powell et al. [37] studied the redox and sorption behaviour of Pu in the presence of magnetite. According to these studies tetravalent actinides sorb strongly at pH values around 4–5, while penta- and hexavalent radionuclides partially reduce to tetravalent species depending on the Fe(II)/Fe(III) ratio at the mineral surface [27]. A good summary of the sorption coefficients for Pu, Am, U, Np and Tc onto Fe hydroxides and oxides was published by Li and Kaplan [28]. Very little literature is available on europium as a chemical analogue of americium and its respective sorption behaviour on magnetite [7,29,45]. Kirsch et al. [26] investigated Pu^{3+} interaction with magnetite and found strong sorption and formation of tridentate inner sphere surface complexes. None of these data sets focuses on environments with high ionic strength (I).

Highly saline solutions can occur at sites near rock salt formations [6,13]. Brine solutions of high ionic strength up to 6.7 m for NaCl [23] have been encountered in repository environments directly located in rock salt formations (e.g. the WIPP site, US; <https://www.wipp.energy.gov/>). Such conditions may affect RN solubility and retention processes in the geochemical barriers. Furthermore, at high salt concentrations, the activity coefficients of aqueous species undergo significant changes. While sorption and reduction behaviour of uranium in the presence of magnetite under reducing saline conditions has been reported by Grambow et al. [15], the effect of ionic strength on trivalent radionuclides sorption onto magnetite has not yet been investigated.

Electrostatic surface complexation modelling (SCM) is a powerful tool that is commonly used to describe the sorption behaviour of RNs on mineral surfaces. SCM is able to consider charges of adsorbing species and adsorbent surfaces and, therefore, also ionic strength effects [30]. Only few studies dealing with sorption of RNs at high I coupled with SCM have been published. Schnurr et al. [43] examined europium sorption onto clay minerals at nearly saturated saline solutions while Ams et al. [2] investigated neptunium sorption onto bacteria under moderately saline conditions. In both cases, a non electrostatic surface complexation model could satisfactorily describe the experimental data. Mahoney & Langmuir [31] modelled previously published experimental data on strontium adsorption to clay minerals and found that the combination of a triple layer model with Pitzer activity coefficients resulted in worse simulations than when applying activity coefficients calculated by

the Davies equation even at 4.0 M NaCl salt level. Most recently, Garcia et al. [14] used a basic Stern model to describe the uptake of europium on quartz up to high NaCl concentrations. This appears to be the first time an electrostatic model has been coupled with a Pitzer approach to describe a self consistent set of experimental data.

For cation sorption to pure oxides it is well known that surface charge and surface electrostatics can play a significant role (e.g. [30]). Therefore, the aim of the present study is to examine the uptake of americium/ europium by magnetite under reducing conditions in background electrolyte NaCl solutions with various I up to 6.67 m . An X ray absorption spectroscopy (XAS) study at the L_3 edge for americium in contact with magnetite in background electrolytes with I of 1 m and 6.5 m NaCl is performed to provide the molecular level information on Am surface speciation at different pH and I to ultimately aid evaluating underlying mechanisms and binding modes. At last, the data are modelled using a charge distribution multi site triple layer surface complexation model (CD MUSIC) starting from magnetite surface hydroxyl acid/base parameters to obtain the complexation constants at infinite dilution. To our knowledge no systematic sorption study, which exhibits the combination of uptake data, modelling and spectroscopic studies of radionuclides onto iron corrosion products in nearly saturated salt solutions is presently available. The newly obtained data will serve as input for performance assessment of radioactive waste disposal under saline ground or porewater conditions.

2. Materials and methods

All reagents (except the RNs) were of analytical grade and used without further purification. Ultrapure water (MilliQ system, 18.2 $\text{M}\Omega/\text{cm}$) was used to prepare suspensions and electrolyte solutions. These were purged with Ar prior to storage in an Ar filled glove box. The atmosphere in the anoxic glove box was CO_2 free with O_2 content below 1 ppmv. All sorption experiments were run in an Ar filled glove box at room temperature. Samples for the XAS study were prepared and encapsulated under Ar and measurements were performed at room temperature under anoxic conditions.

2.1. Magnetite characterization

Magnetite was synthesized following the procedure described by Cornell and Schwertmann [8]. The solid phase was characterized by X ray diffraction (XRD, D8 Advance from Bruker AXS, $\text{Cu K}\alpha$ radiation, Sol X detector), scanning electron microscopy (SEM, Quanta 650 FEG, FEI), energy dispersive X ray spectroscopy analysis (EDX, Thermo Scientific NORAN System 7), and X ray photoelectron spectroscopy (XPS, VersaProbe II, ULVAC PHI, Al $\text{K}\alpha$ monochromatic X ray excitation). The specific surface area of the same batch (40 g/L stock suspension) was previously determined by Finck et al. [12] by the BET method to be 13.1 m^2/g . XRD (Fig. 1B) analysis was performed with the stock suspension and compared to literature data (red colour), showing an excellent match and the absence of additional crystalline phases. The SEM picture in Fig. 1A shows clear octahedral morphology and size range of 50 to 300 nm with average size of 100 nm, while EDX confirmed an Fe/O ratio matching the magnetite ratio $\frac{3}{4}$. The exposed octahedral face also hints at predominance of the (1 1 1) plane as being relevant for sorption. XPS was used to obtain the Fe 2p spectrum of the magnetite stock suspension and shows the presence of both Fe(II) and Fe(III). The respective ratio of $\text{Fe}(\text{II})/\text{Fe}_{(\text{tot.})}$ was 0.25, while in the ideal magnetite structure it should be 0.33. This result may hint at a slight increase in Fe(III) within the first few nm

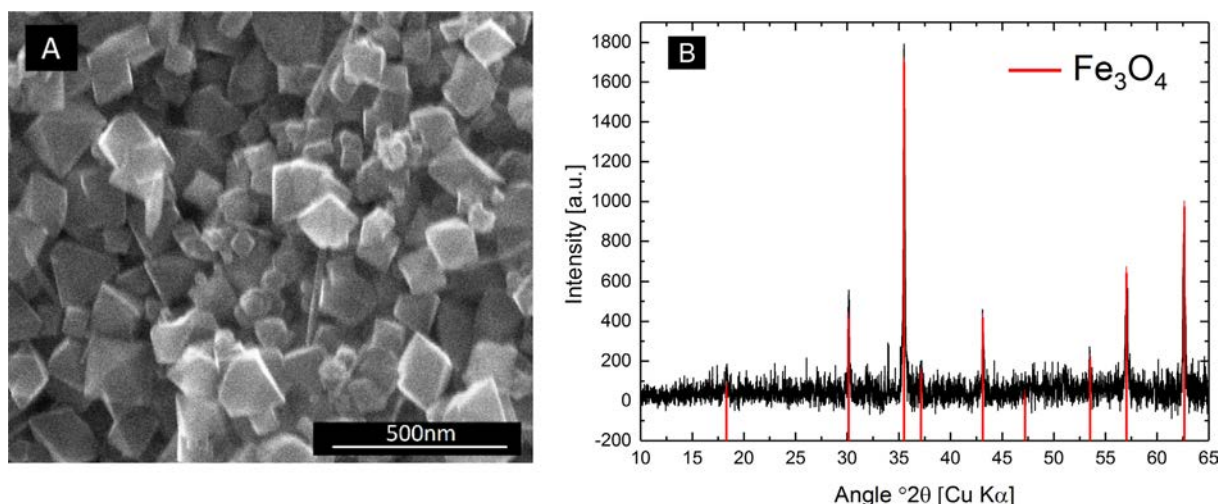


Fig. 1. Scanning electron micrograph (SEM) (A) and X-ray diffractogram (XRD) (B) of the magnetite used in this study (stock suspension). XRD identified the solid phase as magnetite by comparison with jcpds card # 75-0033 (red bars), no other phase is detected. (For interpretation of the references to colour in this figure legend, the reader is referred to the web version of this article.)

probed by XPS and originates from the long contact time between magnetite and the traces of oxygen in Ar filled box. At last, prior to the sorption experiments, it was crucial to identify the stability of magnetite along the pH range to avoid mineral dissolution or phase transformation. Plotting a Pourbaix diagram using the Geochemist workbench (GWB) software (version 8.0) [4,5] showed low solubility for magnetite under reducing conditions in neutral and alkaline range. At $\text{pH}_m > 5.6$ (25) magnetite solubility is relatively low. It is unlikely to affect significantly the sorption experiments performed within a period of 24 h.

2.2. Chemicals

NaCl (99.9% purity) for the background electrolyte preparation, HCl, NaOH for pH adjustment, MES (2 (N morpholino) ethanesulfonic acid) and MOPS (3 (N morpholino) propanesulfonic acid) buffers were obtained from Merck. Radioactive europium was used for batch experiments as a chemical analogue to trivalent actinides. It allowed direct gamma measurements and avoided dilution due to salt content, which would be needed for high resolution (HR) ICP MS (Thermo Element XR). The europium stock solution consisted of dissolved EuCl_3 (Eckert & Ziegler) with a composition of > 95% ^{152}Eu ($t_{1/2} = 13.5$ y), 3.76% ^{153}Gd and 0.55% ^{154}Eu , and had activity of 1×10^4 MBq/L. Inactive europium used alongside active europium for experiments with Eu concentration of 1.2×10^{-5} M was obtained from dissolved Eu_2O_3 . For the XAS study, an Am stock solution with isotopic composition of 99.5% ^{243}Am ($t_{1/2} = 7370$ y), 0.5% ^{241}Am and an activity of 1.11×10^4 MBq/L was used. The concentrations of Am and inactive Eu in the respective stock solutions were confirmed by HR ICP MS.

2.3. Batch sorption experiments

Sorption studies were performed in batch type experiments. Solid liquid distribution coefficients (K_D values) for europium were obtained as a function of pH_m (range 5.6–8.2, step ~ 0.2) at various salt levels for NaCl ($I = 1$ M, 3.5 M, 6.67 M) at constant solid to liquid ratio (0.5 g/L) and fixed Eu concentrations (5.1×10^{-10} M ~ 6×10^{-10} M and 1×10^{-5} M ~ 1.2×10^{-5} M). The pH_m range is limited to 5.6 due to dissolution of magnetite in the acidic range, and to 8.2 due to potential $\text{Eu}(\text{OH})_3$ precipitation at least in the

absence of a sorbent. MES and MOPS buffers (20 mM) were used in all samples to avoid pH drifts.

The pH measurements were done with a Metrohm Solitrode pH electrode with reference electrolyte 3 M KCl. The pH electrode was calibrated using reference buffer solutions of pH 4, 7, and 10 (Radiometer Analytical). The pH was measured for 10 min to allow stabilization and thus get an accurate result. In saline solutions, $I \geq 0.1$ M, all the measured pH_{EXP} values were corrected to molal proton concentration $\log m_{\text{H}^+}$ by use of the A factor as follows:

$$\log[m_{\text{H}^+}/(\text{mol/kg})] = \text{pH}_{\text{EXP}} + A \quad (1)$$

A is a correction term specific for a given electrolyte, is concentration dependent and is calculated from an empirical polynomial for NaCl [1]:

$$A_{\text{NaCl}} = 0.0013 \times (m_{\text{NaCl}})^2 + 0.1715 \times (m_{\text{NaCl}}) - 0.0988 \quad (2)$$

where m is the molality of the background electrolyte. All mentioned pH values refer to the molal concentration of protons ($\log[m_{\text{H}^+}/(\text{mol/kg})] = \text{pH}_m$).

After an equilibration period of 24 h, a given suspension was ultracentrifuged (Beckman Coulter XL 90K) at 90,000 rpm (~700,000 g) for 30 min. After phase separation, the concentration of the radionuclide in the supernatant was quantified using a gamma counter (Packard Cobra Auto Gamma 5003). The supernatant was also analysed by HR ICP MS to quantify the content of dissolved Fe to conclude whether dissolution of magnetite had occurred. The values of dissolved iron reached a maximum of 1% of the initial Fe content at pH_m 5.4, highlighting low dissolution in the used pH range in agreement with the solubility study by Missana et al. [32] and GWB modelling in this study.

Sorption data were evaluated as percentage adsorbed and in terms of the logarithm of the distribution coefficient K_D as a function of pH_m . The distribution coefficient was calculated via:

$$K_D \left\{ \frac{\text{L}}{\text{kg}} \right\} = \frac{C_i - C_e}{C_e} \times \frac{V}{m} \quad (3)$$

here the C_i and C_e are the initial and equilibrium concentrations of europium in the liquid phase and V/m is the ratio of the volume of the solution and the mass of the solid in L/kg.

The sorption isotherm studies followed similar experimental procedure, separation and measurement processes. In the latter,

the uptake of europium sorbed at magnetite surface (in mol/g) was obtained for $I = 1\text{ m}$, 3.5 m , 6.67 m NaCl at constant solid to liquid ratio (0.5 g/L) and Eu concentration ranging from 10^{-4} M to $5 \times 10^{-10}\text{ M}$ at $\text{pH}_m \sim 6$ and ~ 7 . The data was then plotted as a function of Eu concentration in the liquid phase and is shown in Supplementary Information.

2.4. X ray absorption spectroscopy sample preparation & measurements

For the extended X ray absorption fine structure (EXAFS) measurements, four samples were examined at a fixed solid to liquid ratio of 1 g magnetite /L at pH_m values of 6.1 and 7.1 for $I = 1\text{ m}$, as well as 6.3 and 7.2 for $I = 6.5\text{ m}$. The Am concentration was $9.5 \times 10^{-6}\text{ m}$, with MES (20 mM) used to buffer the pH. After an equilibration period of 24 h, the solid phase was transferred into 250 μL PE vials. Am L_3 edge XAS spectra on the solid phase were collected at the KIT synchrotron light source at the INE beamline for actinide science [41]. Energy calibration was done using the Zr K edge XANES of a Zr foil measured along with each sample by assigning the first inflection point to 17998.0 eV. Measurements were done in fluorescence detection mode at room temperature using a 5 element low energy germanium solid state detector (Canberra Eurisys). For each sample, 5–6 scans were recorded to achieve adequate signal to noise ratio. The collected data were analysed and modelled following standard procedures using Athena (Demeter version 0.9.26) and Artemis (version 0.8.012) interfaces of the Iffeffit software [39]. For the four samples of interest, the amplitude reduction factor (S_0^2) was fixed during the fit to the experimental data and set to the value obtained for the americium solution without solid phase used as reference. The coordination number (CN), interatomic distance (ΔR), energy shift (ΔE_0) and Debye Waller term (σ^2) were the fitting parameters for each shell. The k^2 and k^3 weighted Fourier transformed spectra were fitted in R space using a combination of single scattering paths. The misfit between data and model is expressed by the factor F representing the figure of the merit of the fit as defined by Ravel [38].

2.5. Modelling

2.5.1. Speciation and solubility models

PhreeQC (version 3.4.0.12927) [35] was used to obtain the aquatic speciation of Eu/Am and to identify the potential formation of precipitates. For activity corrections, the Harvie Moller Weare Pitzer database [18] and the ThermoChimie database with SIT parameters [16] was used while Neck et al. [34] and Guillaumont et al. [17] provided equilibrium constants and Pitzer and SIT parameters for Eu/Am species, respectively. Both SIT and Pitzer formalisms were compared. The Pitzer (HMW) database does not consider Cl⁻ complexation constants, while SIT reaches the threshold of its validity range at $I \sim 4\text{ m}$.

2.5.2. CD MUSIC model

Surface complexation models have become widely used tools when dealing with mineral surfaces and adsorption of solutes from aqueous solutions. The complexity of the system and objective of the study play an important role when choosing an appropriate model. An electrostatic model was chosen, as it is assumed that even under high ionic strength conditions the electrostatics at metal oxide surfaces due to surface charging cannot be neglected. The various available electrostatic models differ in the treatment of surface charge or the number of planes and sites. Regarding the sorption sites, the CD MUSIC approach, considering multiple sites and charge distributions based on the triple layer model [9] was adopted. This approach developed by Hiemstra & Riemsdijk [20]

treats surface complexes not as point charges located in one electrostatic plane but rather as having a spatial charge distribution in the interfacial region over two electrostatic planes. The MUSIC model is best suited to address the complex crystal structure of magnetite, containing tetrahedral and octahedral configurations alongside different site densities for different crystal faces, and to predict the proton binding constants for the several terminal oxygen sites. Modelling was performed using a modified version of FITEQL 2 [52] with the databases described above. The activity coefficients were obtained from the Pitzer formalism only. In this work, the titration of magnetite was done in solutions with ionic strengths of 0.1 m and 1 m NaCl. A volume of 25 ml of stock suspension giving the exposed surface area of magnetite =14 m² was manually titrated under argon atmosphere, by first adding 35 μL of 1 M NaOH to obtain alkaline conditions and then adding 100 μL of 0.01 M HCl every 2 min and recording the pH until pH around 5 was achieved. It was preferential to start at alkaline conditions to avoid dissolution of magnetite in acidic pH region. The relative charge was then calculated as a function of pH_m . These data were fitted with the constants and site densities from Vaysières [51], who reported the number of possible surface species along with formal charges and structural configuration for the (1 1 1) face of magnetite. The capacitance values and binding constants for Cl⁻ and Na⁺ to variously coordinated sites were obtained from the fit. The constants for Cl⁻ and Na⁺ binding to surface hydroxyl groups were set equal to reduce the number of adjustable. Two different terminations occur in the (1 1 1) plane: the oxygen atoms are either coordinated to iron atoms in octahedral sites or to iron atoms in mixed octahedral and tetrahedral sites. In the octahedral termination the oxygen atoms are doubly and triply coordinated, i.e. two and three metal ions are coordinated to the oxygen, while in the mixed tetrahedral and octahedral termination they are doubly and singly coordinated. Table 1 summarizes the pK values for each coordination.

The contributions from the two terminations were adjusted in such a way that the experimental point of zero charge (pzc) was retrieved. This was done for low ionic strength (1 mM) using a purely diffuse layer model. After the final optimization, the capacitance values and the binding constants within the triple layer model were fixed and the solid amount was adjusted to the europium sorption experiments (0.5 g/L). The model was further modified to account for activity coefficients of europium species in solution with respect to the changing ionic strength. Furthermore, the dielectric constant of solvent (i.e. solutions) was estimated for each ionic strength and used for the diffuse part of the triple layer model. The model was run in various site configurations until a good fit was achieved.

Table 1
pK values for each coordination in two terminations of magnetite taken from Vaysières [51].

Octahedral termination		pK	Surface charge calculated from bond valence		
Coordination of oxo/hydroxo groups	Reaction				
Doubly	$\text{Fe}_2 - \text{O}^{1.16} + \text{H}^+ \rightleftharpoons \text{Fe}_2 - \text{OH}^{0.16}$	16.4	-1.16		
Doubly	$\text{Fe}_2 - \text{OH}^{0.16} + \text{H}^+ \rightleftharpoons \text{Fe}_2 - \text{OH}_2^{0.84}$	2.5	-0.16		
Triply	$\text{Fe}_3 - \text{O}^{0.75} + \text{H}^+ \rightleftharpoons \text{Fe}_3 - \text{OH}^{0.25}$	7.6	-0.75		
Mixed octahedral and tetrahedral termination		pK	Surface charge calculated from bond valence		
Doubly	$\text{Fe}_2 - \text{O}^{0.83} + \text{H}^+ \rightleftharpoons \text{Fe}_2 - \text{OH}^{0.17}$			9.3	-0.83
Doubly	$\text{Fe}_2 - \text{OH}^{0.17} + \text{H}^+ \rightleftharpoons \text{Fe}_2 - \text{OH}_2^{1.17}$			-5.1	0.17
Singly	$\text{Fe}_1 - \text{O}^{1.25} + \text{H}^+ \rightleftharpoons \text{Fe}_1 - \text{OH}^{0.25}$			17.5	-1.25
Singly	$\text{Fe}_1 - \text{OH}^{0.25} + \text{H}^+ \rightleftharpoons \text{Fe}_1 - \text{OH}_2^{0.75}$	3.6	-0.25		

3. Results

3.1. Magnetite titration

The experimental procedure for magnetite titration is explained alongside the model in Section 2.5.2. Fig. 2 shows the experimental titration data for two ionic strengths, 0.1 *m* and 1 *m* NaCl in the pH_m range of 5.3–8.8 and the associated modelled charges. The error bars for the surface charge are within the points. The point of zero charge was found at $pH_m = 6.4$. This is in agreement with various published data summarized in a recent review by Vidojkovic & Rakin [49]. The best model parameters are summarized in Table 2, showing the two capacitance values as well as ion binding constants (Na^+ , Cl^-) to variously coordinated hydroxyl sites. The ion binding constants for anions and cations on a given site were set to identical values. The simplest model in terms of numbers of adjustable parameters using equations in Table 1 was obtained when enforcing identical intrinsic ion binding constants for singly and triply coordinated sites and a separate value for the doubly coordinated sites. The fitted value for the doubly coordinated sites is very low which indicates that ion binding on these sites is rather weak. Overall, the procedure reduced the number of ion binding constants from 8 to 2. The overall Stern capacitance value of 1.32 F/m^2 is within the range for overall capacitance for metal (hydr)oxides reported by Hiemstra & Van Riemsdijk [19] for non porous and well ordered planar crystal faces from 0.9 to 1.7 F/m^2 .

3.2. Batch sorption investigation

3.2.1. Europium and americium aqueous speciation and solubility

In order to assess the dominant species of europium/ americium in the aqueous solution for modelling, speciation diagrams were obtained with Phreeqc using the ThermoChimie database with the SIT parameters [16] at various ionic strengths (1 *m*–6.67 *m* NaCl) corresponding to those used in the sorption experiments (Fig. 3). The same calculations were performed using the Pitzer formalism and compared.

For the region of interest, pH_m 5–8, the dominant species for europium are Eu^{3+} and $EuCl_2^{2+}$ according to the calculations. Their proportions depend on the NaCl concentration. $EuCl_2^{2+}$ becomes dominant at $I \geq 3.5$ *m*. Beyond pH_m 7.5 for $I = 1$ *m* and $I = 6.67$ *m*, the fraction of chloride complexes start to drop and at

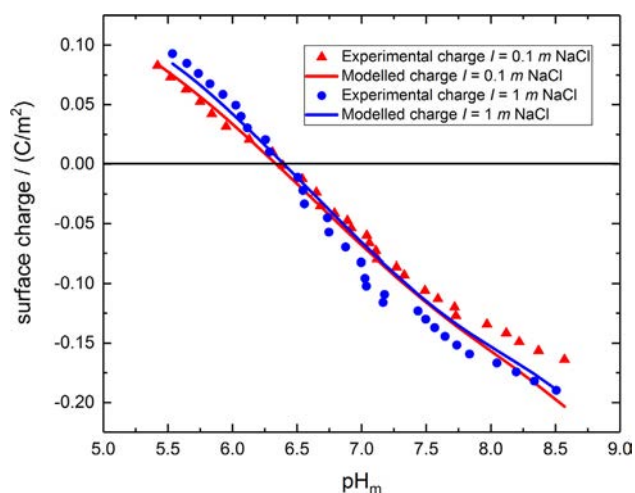


Fig. 2. The experimental and modelled charging behaviour of magnetite at two ionic strengths set by NaCl. The lines correspond to the calculated charges using the values summarized in Table 2.

Table 2

The CD-MUSIC model parameters for magnetite proton surface charge curves.

Capacitance 1	3.22	F/m^2
Capacitance 2	2.25	F/m^2
Overall Stern capacitance	1.32	F/m^2
Constant for Cl^- and Na^+ binding to doubly coordinated hydroxyl sites, log K_a	-5.01	-
Constant for Cl^- and Na^+ binding to singly/triply coordinated hydroxyl sites, log K_e	2.45	-
Site densities used in optimization		
Doubly coordinated octahedral termination	6.68	sites/ nm^2
Triply coordinated octahedral termination	2.23	sites/ nm^2
Singly coordinated mixed termination	1.48	sites/ nm^2
Doubly coordinated mixed termination	4.45	sites/ nm^2

$pH_m \geq 8.5$, $Eu(OH)_2^{2+}$ and $Eu(OH)_3^{2+}$ gain significance. Increasing the Eu concentration to 1.2×10^{-5} *m* yields the same speciation for all ionic strengths. Speciation diagrams were calculated for americium following the same process.

The ionic strength effect on the aqueous speciation of Am differs from that of Eu. The Am^{3+} aquo ion is dominant as a single species up to pH_m 7.0 for $I = 1$ *m*. At pH_m 8.0, in addition to Am^{3+} , $Am(OH)_2^+$ and $Am(OH)_2^{2+}$ become significant. With increasing ionic strength to $I = 6.5$ *m*, Am^{3+} dominates along with $AmCl_2^{2+}$ up to pH_m 7.2. For $pH_m > 7.7$, $Am(OH)_2^+$ and $Am(OH)_2^{2+}$ increase as in the low I case. Speciation curves calculated using the Pitzer formalism are similar to those obtained by using SIT at low $I = 1$ *m*, however for $I = 6.5$ *m*, Am^{3+} is the dominant species up to pH_m 7.2, where $Am(OH)_2^{2+}$ intensity reaches 30% and takes over. The reason is that parameters for $AmCl_2^{2+}$ / $AmCl_2^+$ species are missing for NaCl solution in the Pitzer database. The dominant species in aqueous solution at pH_m 6.4 where europium sorption becomes dominant are Eu^{3+} and $EuCl_2^{2+}$. Under those conditions, existing data sets suggest americium existing solely as Am^{3+} aquo ion. The speciation curves for Eu at $I = 3.5$ *m* and Am for all I of interest are available in the Supplementary Information.

An important aspect prior to starting experiments was to assess the potential precipitation of any solid phase under the studied conditions. This was established by plotting the saturation indices of relevant solid phases as a function of pH_m at various ionic strengths for europium (Fig. 4). In the case of a Eu concentration of 6×10^{-10} *m*, the precipitation of $Eu(OH)_3(cr)$ starts at pH_m 9.5 for $I = 1$ *m* (Fig. 4 left), and at pH_m 11.8 for $I = 6.67$ *m* (Fig. 4 right). Crystalline phases are not expected to form under our experimental conditions, but the saturation indices of these were considered to be on the conservative site. Amorphous solid phases such as $Eu(OH)_3(am)$, however, should not precipitate within the entire pH_m range investigated. Additional calculations were performed at Eu concentration of 1.2×10^{-5} *m* where sorption studies were also performed (Figures in Supplementary Information). According to those calculations, precipitation of $Eu(OH)_3(cr)$ is expected to start already at $pH_m = 7.4$ for $I = 1$ *m* and $Eu(OH)_3(am)$ as well as $EuCl(OH)_2(s)$ are predicted to precipitate at $pH_m > 8.0$. When increasing the ionic strength to $I = 6.67$ *m*, the solution becomes oversaturated with regard to $Eu(OH)_3(cr)$ at $pH_m > 8.0$ and $EuCl(OH)_2(s)$ at $pH_m > 8.2$, respectively.

In the case of americium, the saturation index at $I = 1$ *m* at a metal ion concentration of 9.5×10^{-6} *m* at pH_m 6.1 and 7.1 remains below 0 and only becomes positive for $Am(OH)_3(cr)$ at $pH_m > 7.5$ and thus no precipitation is expected to occur in samples prepared for XAS measurements, where this Am concentration is used. Increasing I to 6.5 *m*, $Am(OH)_3(cr)$ is expected to precipitate at $pH_m > 8.4$. Thus, I shifts the precipitation threshold to the alkaline region on the pH_m scale. For all solutions, NaCl is below saturation and no precipitation of halite is taking place. Other solid phases such as $AmCl_3$, or Am_2O_3 were considered but did not come close

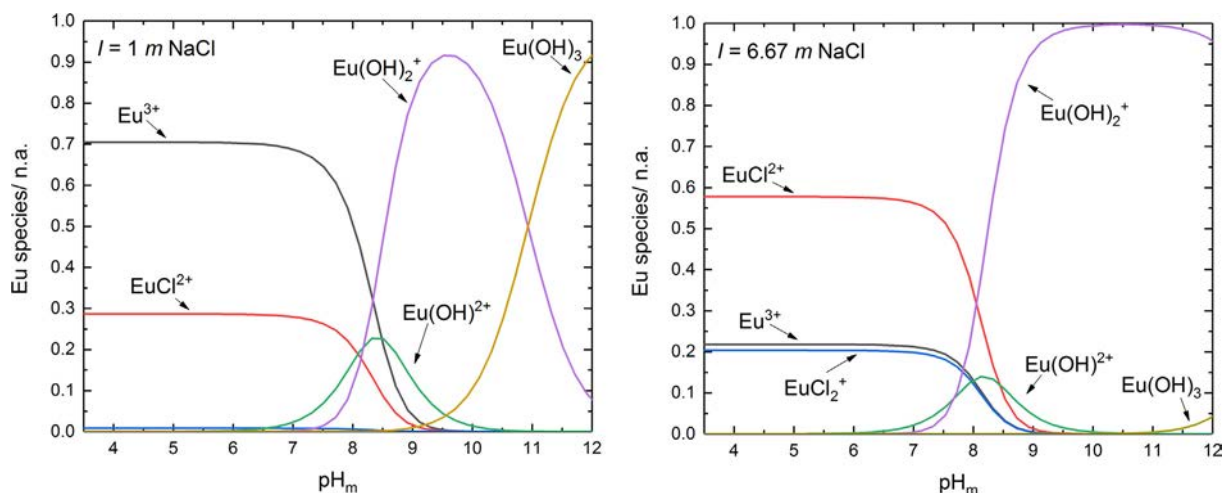


Fig. 3. Aqueous speciation of europium vs pH_m calculated using the SIT database. $I = 1 \text{ m NaCl}$ (left) and $I = 6.67 \text{ m NaCl}$ (right), $[\text{Eu}] = 6 \times 10^{-10} \text{ m}$.

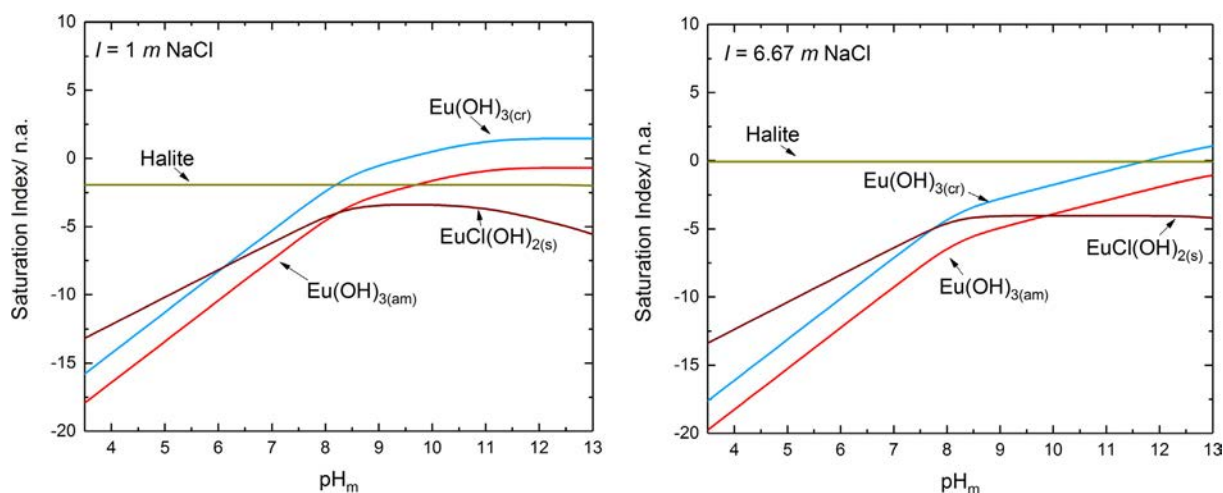


Fig. 4. Saturation indices of europium solid phases vs pH_m calculated using the SIT database. $I = 1 \text{ m NaCl}$ (left) and $I = 6.67 \text{ m NaCl}$ (right), $[\text{Eu}] = 6 \times 10^{-10} \text{ m}$.

to precipitation within the whole pH_m range for all I . The saturation indices of americium vs pH_m are shown in the Supplementary Information.

3.2.2. Sorption of europium as a function of pH

The pH dependent sorption of trivalent radionuclides (Eu) to iron oxides exhibits, as expected, strong sorption above pH_m 5.6 (Fig. 5 *left*). At low Eu concentration, $6 \times 10^{-10} \text{ m}$, the increasing salt content does not show any substantial effect and almost complete uptake (>99.5%) is observed for the investigated ionic strength range for $\text{pH}_m \geq 6.4$. The $\log K_D$ values range from 4.9 to 7.0 (Fig. 5 *right*), with $\log K_D$ values at pH_m 6.4 of 6.7 ± 0.5 at $I = 1 \text{ m}$ and 5.2 ± 0.5 at $I = 6.67 \text{ m}$. Gamma counting yields only small analytical uncertainties. Errors due to pipetting, resuspension of solid particles after ultracentrifugation or wall sorption effects dominate the uncertainty of sorption data. The uncertainty of $\log K_D$ values by all these errors is around ± 0.5 , which is in agreement with data provided by Schnurr et al. [43]. The grey area in the figures illustrates the detection limit of the gamma counting method and corresponds to 99.99% sorption. The $\log K_D$ value corresponding to this uptake is above 7.5.

Singh et al. [45] investigated the sorption of europium onto magnetite for a Eu concentration of $2 \times 10^{-9} \text{ M}$. They observed a similar trend with almost complete sorption at $\text{pH}_m > 5.5$

($I = 0.1 \text{ M}$). Those authors used magnetite with a higher specific surface area in comparison to the magnetite used in this study.

Sorption data were recorded at a higher concentration of $[\text{Eu}] = 1.2 \times 10^{-5} \text{ m}$ corresponding closely to the concentration of Am chosen for XAS experiments. The sorption exhibited a pH_m dependent behaviour. The uptake was low at pH_m 5.6 and increased rapidly within 2 pH_m units, reaching almost complete sorption at $\text{pH}_m \sim 8$ (Fig. 6 *left*). At this Eu concentration, a small ionic strength effect can be observed. The $\log K_D$ in this case varies from 2.7 ± 0.2 at 20% sorption to 4.6 ± 0.2 at 95% sorption (Fig. 6 *right*). The uncertainty regarding sorption was estimated in this case $\pm 4\%$, i.e. ± 0.2 for $\log K_D$. These experimental data are in good agreement with work of Catalette et al. [7], who performed europium sorption onto magnetite at a Eu concentration of $2 \times 10^{-4} \text{ M}$ and observed >99.99% uptake at $\text{pH}_m > 7.0$ at $I = 0.1 \text{ M}$.

3.3. Americium X ray absorption spectroscopy and coordination geometry

EXAFS measurements allow exploring the in situ molecular structure of surface species. In order to obtain the amplitude reduction factor, reference Am^{3+} aquo ions were modelled, fitting the data with one O coordination shell containing $\text{CN}_{\text{O}1} = 9.0$ atoms (parameter was set) at a distance of $R(\text{Am O}1) = 2.44 \text{ \AA}$ (Fig. 7,

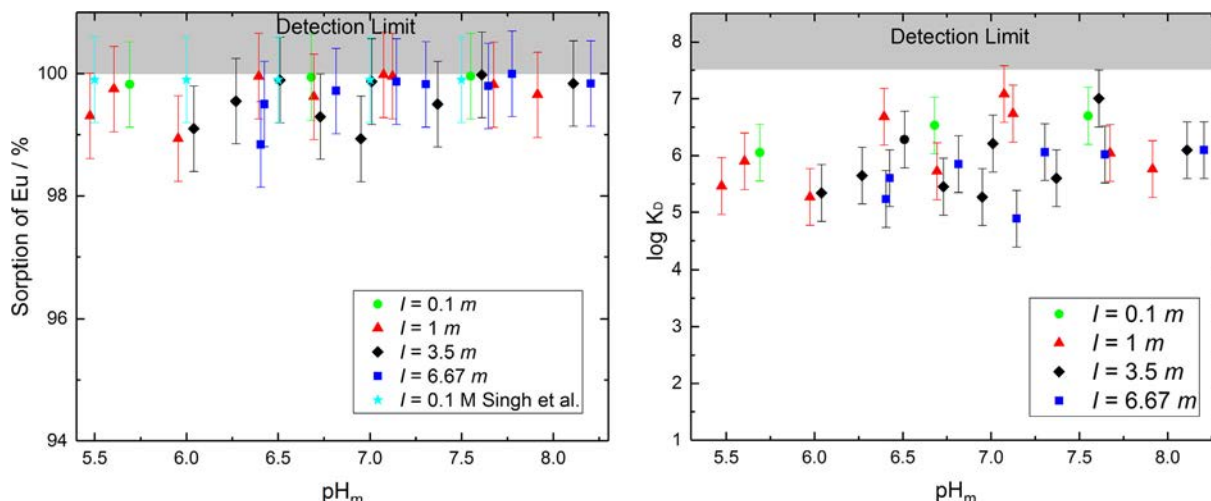


Fig. 5. Data for europium $[Eu] = 6 \times 10^{-10} \text{ M}$ sorption to magnetite as percentage uptake (left) and as logarithm of the distribution ratio ($\log K_D$) (right) as a function of pH_m and at different ionic strengths (NaCl).

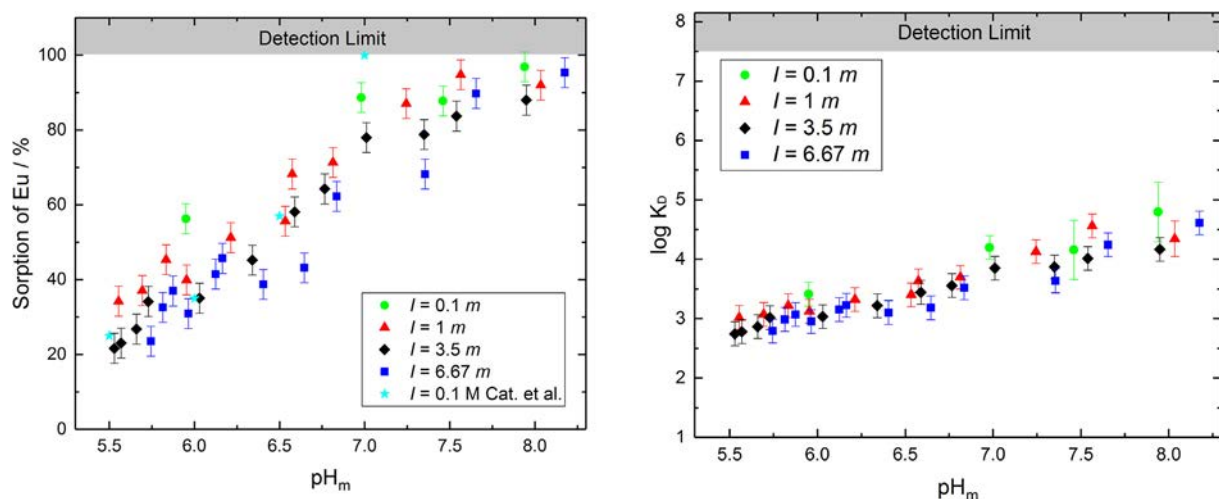


Fig. 6. Data for europium $[Eu] = 1.2 \times 10^{-5} \text{ M}$ sorption to magnetite as percentage uptake (left) and as logarithm of distribution ratio ($\log K_D$) (right) as a function of pH_m and at different ionic strengths of NaCl.

Table 3), in agreement with literature data [46,10]. Samples containing magnetite showed, as expected, different EXAFS spectra at $R + \Delta R > 2.5 \text{ \AA}$ in comparison to those of the aquo ion, highlighting the presence of an ordered shell at higher distances, presumably iron. However, the EXAFS spectra were very similar for all sorption samples, suggesting a similar coordination environment at different pH_m and I . As observed for the calculated aqueous speciation, the dominant aqueous species in sorption samples don't vary significantly between pH_m 6.1 and 7.2 as suggested by EXAFS for sorbed americium. Experimental and modelled EXAFS data are shown in Fig. 7, and the model parameters are summarized in Table 3.

There is one contribution in the Fourier transformed spectra for aquo ions and two contributions for the sorption samples. The refinement yields 9(1) oxygen atoms in the first coordination sphere of Am for all samples, where O atoms are located at the distance of 2.48–2.53 Å (Table 3). In order to obtain further information about the structure of Am species on magnetite, the fit was extended to the Fourier transform peak beyond the oxygen coordination sphere. The refinement of the second shell in the FT data at $R + \Delta R = 3.35 \text{ \AA}$ yields an Am-Fe interaction where the peak was fitted with 3(1) Fe atoms at a distance of 3.49–3.54 Å. This implies

that an Am atom is linked via three oxygen atoms to three edge sharing FeO_6 octahedra, as shown in Fig. 8, with six remaining oxygen atoms in the liquid phase. This is in agreement with the work of Kirsch et al. [26], who examined Pu^{3+} sorption onto magnetite at low $I = 0.1 \text{ M NaCl}$ and with the data reported by Finck et al. [11,12], who examined Am sorption onto magnetite at low I (0.1 M NaCl). The latter authors observed the formation of the same monomeric tridentate inner sphere surface complex highlighting the similarity of the Am surface species structure for data obtained at low and high I , which confirms the negligible effect of I on the structure of surface complexes. No neighbouring Am atoms were detected, excluding the presence of precipitates at the surface. The absence of precipitates is consistent with PhreeqC precipitation calculations. Adding a Cl coordination shell which might be expected as a consequence of Am chloro complex formation at high Cl⁻ concentration did not improve the fit. Thus, the presence of the chloride complex at the magnetite surface was considered insignificant under our experimental conditions.

Different literature data suggest that if americium would be present during the formation of magnetite from Fe(0) , it might substitute for iron in early stages and once the magnetite phase

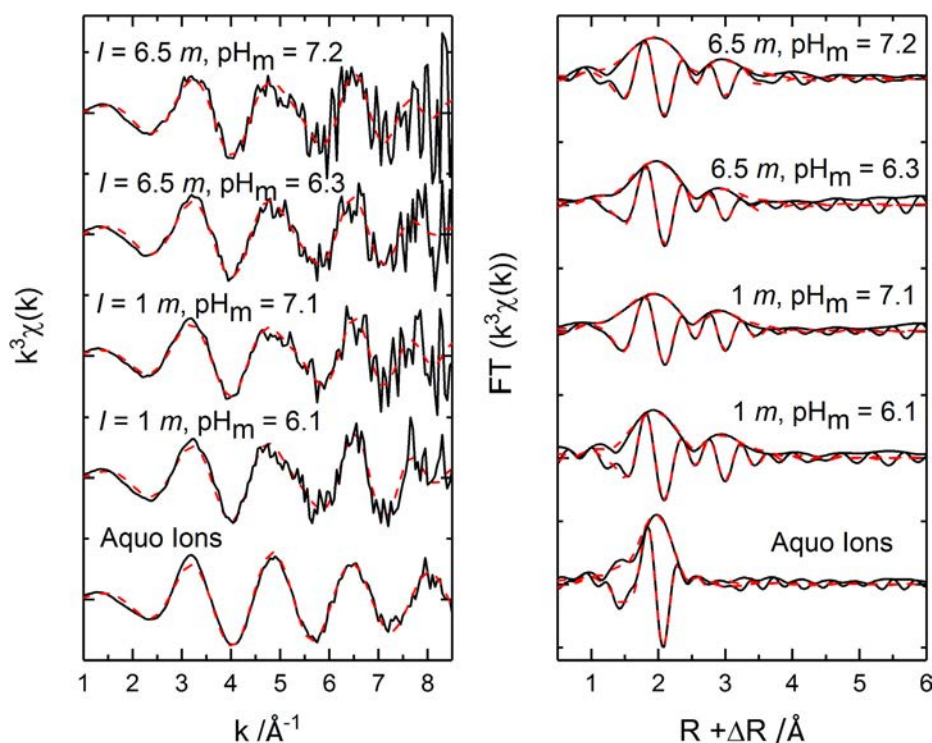


Fig. 7. Experimental (black solid line) and modelled (red dashed line) EXAFS spectra in k space (left) and Fourier transforms (right) of the Am^{3+} aquo ions and sorption samples. Fit results are presented in Table 3. (For interpretation of the references to colour in this figure legend, the reader is referred to the web version of this article.)

Table 3

Best-fit EXAFS Model Parameters for americium sorbed onto magnetite and the reference compound (Am^{3+} in solution).

Sample	FT range [\AA^{-1}]	Fit range in R space [\AA]	Path	CN	R [\AA]	σ^2 [\AA^2]	ΔE_0 [eV]	Factor F
Am^{3+} Aquo ions	3.2–10.3	1.7–2.6	Am-O1	9.0	2.44	0.008	1.2(1.4)	0.0021
Am-Magnetite, pH_m 6.1, $l = 1$ m	3.2–8.2	1.5–3.5	Am-O1	8.9(6)	2.51	0.011	1.8(1.3)	0.0013
Am-Magnetite, pH_m 7.1, $l = 1$ m	3.2–7.8	1.3–3.45	Am-O1	9.9(7)	2.48	0.016	0.1(1.1)	0.0019
Am-Magnetite, pH_m 6.3, $l = 6.5$ m	3.3–8.0	1.35–3.3	Am-O1	9.6(9)	2.53	0.013	2.5(2.1)	0.0018
Am-Magnetite, pH_m 7.2, $l = 6.5$ m	3.2–7.7	1.3–3.3	Am-O1	9.9(6)	2.49	0.015	1.9(0.5)	0.0019
			Am-Fe1	2.5(9)	3.54	0.008		
			Am-Fe1	3(2)	3.49	0.006		
			Am-Fe1	3.1(5)	3.53	0.006		
			Am-Fe1	2.9(6)	3.54	0.007		

FT: Fourier Transform range, CN: Coordination number, R: Interatomic distance, σ^2 : Debye – Waller factor, ΔE_0 : Shift in ionization energy where E_0 is the energy at the maxima of the first derivative, F factor: figure of merit of the fit representing the absolute misfit between the data and the model. Amplitude reduction factor $S_0^2 = 0.87$ for all samples. Estimated error for R = ± 0.03 \AA and for $\sigma^2 = \pm 0.001$ \AA^2 . The numbers in parentheses indicate the uncertainty.

is formed, it would be localized within its structure [11]. A comparison of our data with reported EXAFS data for structurally incorporated americium exclude such retention mechanism in the present study.

3.4. Americium CD MUSIC triple layer model

The developed surface complexation model is based on the aquatic speciation of europium/ americium as presented in Section 3.2.1, the magnetite surface structural model (Tables 1 and 2) and the EXAFS characterization of the surface complex structure obtained for americium. Substituting europium with americium does not have an effect on the model. The surface of the Fe_3O_4 (1 1 1) plane was optimized with either mixed octahedral and tetrahedral termination or only octahedral termination to compare the two terminations as explained in Sections 2.5.2 and 3.1. The spectroscopic results show that the binding mode is tridentate and hence this was included in the model.

The charge distribution in the americium surface complex coordinated by nine oxygen atoms in the model was formulated such that three oxygen bonds would go to the surface and the remaining six were split such that three would be placed in the b plane and three equally divided between the 0 and the b plane to best represent the positioning of americium. This assumption is in agreement with the EXAFS data.

The model provided a very poor fit when using only singly coordinated sites, which was surprising as titration experiments showed these as the dominant sites for proton adsorption. The fit was improving as the distribution of the sites in the model was moving more towards doubly coordinated sites with the best fit if only doubly coordinated sites were used. The doubly coordinated site fit was good for both terminating hydroxyl groups. The spectroscopic data suggest that the binding occurs at the octahedral termination. The result of fitting sorption data by assuming this surface species as relevant is shown in Fig. 9. This configuration matches well with the structure of the octahedral termination

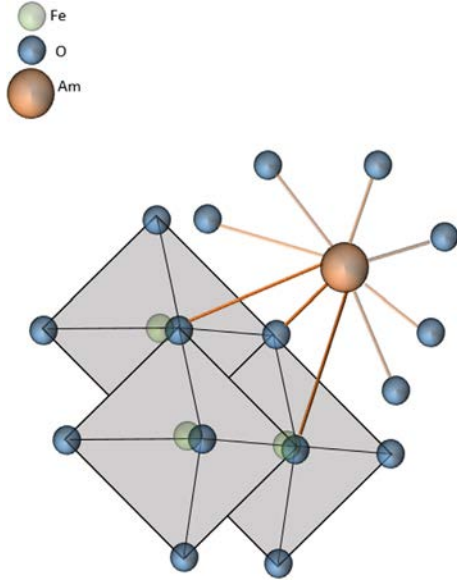
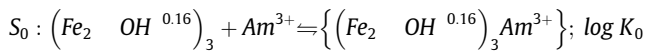


Fig. 8. Sorption complex of Am^{3+} on the edge sharing octahedral (1 1 1) plane of magnetite.

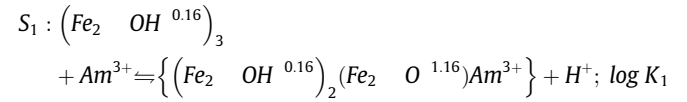
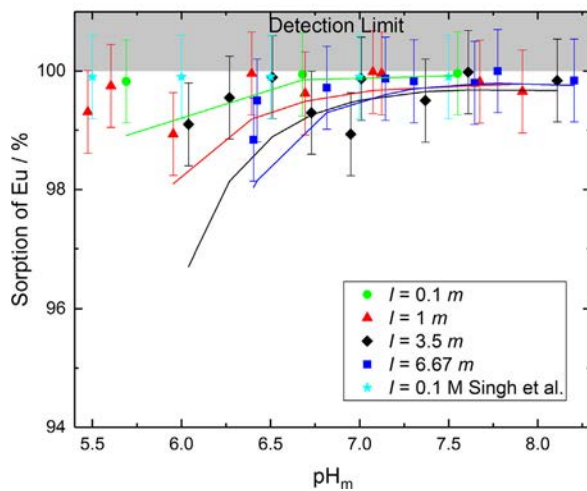
given by Vayssières [51] allowing Am to be located close to three Fe atoms with the same distances and three available O atoms, likewise at the same distances, which is not the case for the mixed termination. The model inherent surface complexes with the associated charge transfers in 0 and β planes are shown below with the complexation constants at infinite dilution summarized in Table 4:



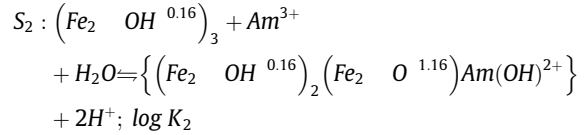
Transfer of charge: $\Delta z_0 = 1.5$, $\Delta z_\beta = 1.5$.

Table 4
The complexation constants at infinite dilution.

$\log K_0$	6.9 ± 0.1
$\log K_1$	0.2 ± 0.1
$\log K_2$	-7.5 ± 0.1



$\Delta z_0 = 0.5$, $\Delta z_\beta = 1.5$.



$\Delta z_0 = 0.5$, $\Delta z_\beta = 0.5$.

Although the aquatic speciation of europium and americium contains significant contributions of $\text{AmCl}^{2+}/\text{EuCl}^{2+}$ species, these seem to be limited to the aqueous solution and do not contribute in significant manner to the surface complexation. The model was fitting well without the introduction of the Am Cl surface complex $\{(\text{Fe}_2 \text{ OH}^{0.16})_3 \text{ AmCl}\}$. The log of the formation constant of species S_1 subtracted from species S_2 is -7.7 . This value is close to log K for americium hydrolysis in solution (-7.2), showing that obtained values are realistic.

The model is able to describe experimental sorption data obtained at different Eu concentration and ionic strengths and as well the respective pH_m dependent trend of sorption (Fig. 9). The model fit for sorption isotherm data is shown in the Supplementary Information.

Fig. 9 also shows the distribution of the different surface complexes as a function of pH_m for $[\text{Eu}] = 1.2 \times 10^{-5} \text{ m}$, where S_0 corresponds to the $\{(\text{Fe}_2 \text{ OH}^{0.16})_3 \text{ Am}^{3+}\}$ complex, S_1 to the $\{(\text{Fe}_2 \text{ OH}^{0.16})_2 (\text{Fe}_2 \text{ O}^{1.16}) \text{ Am}^{3+}\}$ complex, and S_2 to the $\{(\text{Fe}_2 \text{ OH}^{0.16})_2 (\text{Fe}_2 \text{ O}^{1.16}) \text{ Am}(\text{OH})^{2+}\}$ complex. The dashed red lines correspond to surface complex distributions for $I = 1 \text{ m}$, while the dashed blue lines correspond to surface complex distributions for $I = 6.67 \text{ m}$. Considering $I = 1 \text{ m}$, S_0 prevails at low pH_m only up to $\text{pH}_m 5.8$, S_1 exists within the entire studied pH_m range and the hydrolysed S_2 is dominant at high pH_m . Increasing the ionic strength to 6.67 m , the distribution trend is the same, but the dominance of each complex is shifted to higher pH_m , with S_0 being dominant up to $\text{pH}_m 6.6$, and S_1 up to $\text{pH}_m 7.8$. For the clarity, the distribution was not plotted for low europium concentrations of $6 \times 10^{-10} \text{ m}$. In this case the distribution was different with

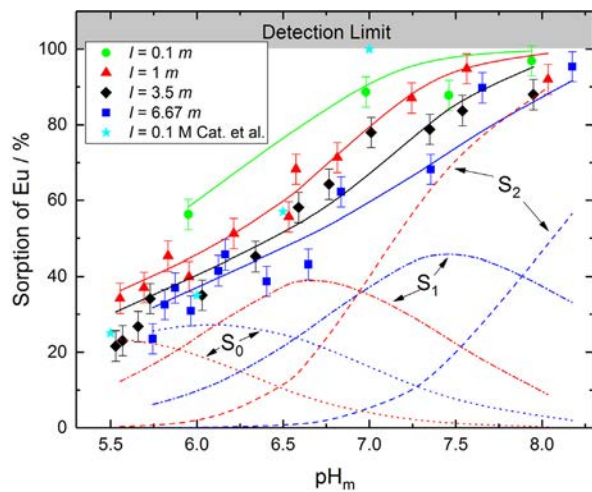


Fig. 9. Sorption of $[\text{Eu}] = 6 \times 10^{-10} \text{ m}$ (left) and $1.2 \times 10^{-5} \text{ m}$ (right) onto magnetite vs pH_m . Experimental uptake (points) modelled (full lines) using surface complexation model in FITEQL with Pitzer database for various ionic strengths (NaCl). The dashed lines represent the complex distribution for the three complexes for $I = 1 \text{ m}$ (red) and $I = 6.67 \text{ m}$ (blue), respectively. (For interpretation of the references to colour in this figure legend, the reader is referred to the web version of this article.)

complex S_0 dominating in the whole pH_m range for $I = 1\ m$ and up to $pH_m\ 7.7$ for $I = 6.67\ m$. The reason for different ionic strength effects for the two various Eu concentrations is the interplay of competition for sites and ionic strength effect on activities in solution. With higher ionic strength the electrolyte interacts with surface sites thus competes with Eu and at higher Eu concentration, this effect is notable. With low Eu concentration, this role of competition is minor. It is worth noting that even at high Eu concentrations only about 59% of the surface sites are occupied. This reflects the high sorption capacity of magnetite, rendering the corrosion phase a candidate for strong radionuclide retention in a nuclear waste repository near field.

4. Conclusions and environmental implications

In this paper, europium/americium binding to magnetite is consistently studied and quantified by batch sorption techniques, spectroscopic characterisation of surface complex structures and surface complexation modelling. The data have resulted in a number of observations, with high relevance concerning the adsorption of trivalent radionuclides on magnetite from aqueous solution up to high salt concentrations. The major outcomes can be summarized as follows:

The pH_m dependent europium sorption is not significantly affected by salinity. Increasing the ionic strength from $1\ m$ to $6.67\ m$ did not result in significant changes in uptake for europium concentration of $6 \times 10^{-10}\ m$. A slight decrease in uptake with increasing ionic strength was observed for europium concentration of $1.2 \times 10^{-5}\ m$.

Even at high salinity, EXAFS indicates that surface speciation does not change and no ternary Am Cl surface complex is present in significant quantities. The studies further demonstrate tridentate binding mode of trivalent radionuclides at the Fe_3O_4 (1 1 1) surface.

Potentiometric titration data of magnetite and experimentally obtained europium uptake can be modelled consistently using a CD MUSIC triple layer model for different metal ion concentrations and ionic strengths up to those in saturated NaCl brines. This model provided complexation constants for three surface complexes, considering sorption of Am^{3+}/Eu^{3+} at the octahedral termination of magnetite on doubly coordinated sites. The data from the titration modelling can be used to model sorption of higher valent actinides as well as other pollutants in solutions up to high ionic strength. The CD MUSIC model allows including more realistic parameters and in depth understanding of the sorption of trivalent radionuclides onto magnetite surface compared to available literature, especially at different levels of ionic strength [7,29,45,26].

It is clearly shown that for the conditions, which are relevant for a nuclear waste repository in saline systems [25], magnetite as the major corrosion product can severely limit the mobility of trivalent actinides and lanthanides in the absence of additional complexing agents such as carbonates. High salinity does not influence this sorption behaviour. This finding shows that many parameters regarding sorption obtained at low ionic strength can be applied in performance assessment also for cases in highly saline conditions. Investigations of radionuclide sorption in solutions of more complex composition as e.g. the presence of carbonate are still needed to verify the potential role of magnetite for radionuclide immobilisation in a repository near field.

CRedit authorship contribution statement

Nikoleta Morelová: Validation, Formal analysis, Investigation, Writing original draft, Visualization. **Nicolas Finck:** Conceptualization, Methodology, Writing review & editing, Supervision.

Johannes Lützenkirchen: Methodology, Software, Formal analysis, Writing review & editing. **Dieter Schild:** Formal analysis, Investigation. **Kathy Dardenne:** Software, Formal analysis. **Horst Geckeis:** Conceptualization, Resources, Writing review & editing, Supervision.

Declaration of Competing Interest

The authors declare that they have no known competing financial interests or personal relationships that could have appeared to influence the work reported in this paper.

Acknowledgements

We would like to thank F. Geyer (KIT INE) for the Inductively Coupled Plasma mass Spectrometry Measurements (ICP MS) measurements and Dr. Vanessa Montoya (KIT INE) for modelling advice. We acknowledge the KIT synchrotron light source for provision of instruments at their beamlines and we would like to thank the Institute for Beam Physics and Technology (IBPT) for the operation of the storage ring, the Karlsruhe Research Accelerator (KARA). This work has been supported within the framework of the KORSO project, funded by the German Federal Ministry of Economic Affairs and Energy (BMWi) under contract no. 02 E 11496 B.

References

- [1] M. Altmaier, V. Metz, V. Neck, R. Müller, T. Fanghänel, Solid-liquid equilibria of $Mg(OH)_2(cr)$ and $Mg_2(OH)_3Cl \cdot 4H_2O(cr)$ in the system Mg-Na-H-OH-Cl- H_2O at $25^\circ C$, *Geochim. Cosmochim. Acta* 67 (19) (2003) 3595–3601, [https://doi.org/10.1016/S0016-7037\(03\)00165-0](https://doi.org/10.1016/S0016-7037(03)00165-0).
- [2] D. Ams, J. Swanson, J. Szymanowski, J. Fein, M. Richmann, D. Reed, The effect of high ionic strength on neptunium (V) adsorption to a halophilic bacterium, *Geochim. Cosmochim. Acta* 110 (2013) 45–57, <https://doi.org/10.1016/j.gca.2013.01.024>.
- [3] D. Bennett, R. Gens, Overview of European concepts for high-level waste and spent fuel disposal with special reference waste container corrosion, *J. Nucl. Mater.* 379 (1–3) (2008) 1–8, <https://doi.org/10.1016/j.jnucmat.2008.06.001>.
- [4] C.M. Bethke, *Geochemical reaction modeling*, Oxford University Press, New York, 1996, p. 111.
- [5] C.M. Bethke, S. Yeakel, *The Geochemists' Workbench User's guides, Version 11 Aqueous*, Solutions LLC, Champaign, 2018.
- [6] W. Brewitz Zusammenfassender Zwischenbericht, GSF T 114, 1980.
- [7] H. Catalette, J. Dumonceau, P. Ollar, Sorption of cesium, barium and europium on magnetite, *J. Contam. Hydrol.* 35 (1–3) (1998) 151–159, [https://doi.org/10.1016/S0169-7722\(98\)00123-5](https://doi.org/10.1016/S0169-7722(98)00123-5).
- [8] R.M. Cornell, U. Schwertmann, *The Iron Oxides*, VCH, New York, 1996.
- [9] J. Davis, R. James, J. Leckie, Surface ionization and complexation at the oxide/water interface, *J. Colloid Interface Sci.* 63 (3) (1978) 480–499, [https://doi.org/10.1016/S0021-9797\(78\)80009-5](https://doi.org/10.1016/S0021-9797(78)80009-5).
- [10] N. Finck, K. Dardenne, H. Geckeis, $Am(III)$ coprecipitation with and adsorption on the smectite hectorite, *Chem. Geol.* 409 (2015) 12–19, <https://doi.org/10.1016/j.chemgeo.2015.04.020>.
- [11] N. Finck, S. Nedel, K. Dideriksen, M. Schlegel, Trivalent Actinide Uptake by Iron (Hydr)oxides, *Environ. Sci. Technol.* 50 (19) (2016) 10428–10436, <https://doi.org/10.1021/acs.est.6b02599>.
- [12] N. Finck, L. Radulescu, D. Schild, M. Rothmeier, F. Huber, J. Lützenkirchen, T. Rabung, F. Heberling, M. Schlegel, K. Dideriksen, S. Nedel, H. Geckeis, XAS signatures of $Am(III)$ adsorbed onto magnetite and maghemite, *J. Phys. Conf. Ser.* 712 (2016), <https://doi.org/10.1088/1742-6596/712/1/012085> 012085.
- [13] P. Fritz, S.K. Frappe, Saline groundwaters in the Canadian shield – a first overview, *Chem. Geol.* 36 (1982) 179–190, [https://doi.org/10.1016/0009-2541\(82\)90045-6](https://doi.org/10.1016/0009-2541(82)90045-6).
- [14] D. García, J. Lützenkirchen, V. Petrov, M. Siebentritt, D. Schild, G. Lefèvre, T. Rabung, M. Altmaier, S. Kalmykov, L. Duro, H. Geckeis, Sorption of $Eu(III)$ on quartz at high salt concentrations, *Colloids Surf., A* 578 (2019), <https://doi.org/10.1016/j.colsurfa.2019.123610> 123610.
- [15] B. Grambow, E. Smailos, H. Geckeis, R. Müller, H. Hentschel, Sorption and reduction of uranium(VI) on iron corrosion products under reducing saline conditions, *Radiochim. Acta* 74 (1996) 149–154, <https://doi.org/10.1524/ract.1996.74.special-issue.149>.

- [16] M. Grivé, L. Duro, E. Colàs, E. Giffaut, Thermodynamic data selection applied to radionuclides and chemotoxic elements: an overview of the ThermoChimie-TDB, *Appl. Geochem.* 55 (2015) 85–94, <https://doi.org/10.1016/j.apgeochem.2014.12.017>.
- [17] R. Guillaumont, F. Mompean, T. Fanghangel, V. Neck, J. Fuger, D. Palmer, I. Grenthe, M. Rand, F. Mompean, M. Illemassene, C. Domenech-Orti, K. Ben-Said, Update on the chemical thermodynamics of uranium, neptunium, plutonium, americium and technetium, Nuclear energy agency organisation for economic co-operation and development, Amsterdam, 2003.
- [18] C. Harvie, N. Møller, J. Weare, The prediction of mineral solubilities in natural waters: The Na-K-Mg-Ca-H-Cl-SO₄-OH-HCO₃-CO₃-CO₂-H₂O system to high ionic strengths at 25°C, *Geochim. Cosmochim. Acta* 48 (4) (1984) 723–751, [https://doi.org/10.1016/0016-7037\(84\)90098-X](https://doi.org/10.1016/0016-7037(84)90098-X).
- [19] T. Hiemstra, W. Van Riemsdijk, Physical chemical interpretation of primary charging behaviour of metal (hydr)oxides, *Colloids Surf.* 59 (1991) 7–25, [https://doi.org/10.1016/0166-6622\(91\)80233-E](https://doi.org/10.1016/0166-6622(91)80233-E).
- [20] T. Hiemstra, W. Van Riemsdijk, A surface structural approach to ion adsorption: the charge distribution (CD) model, *J. Colloid Interface Sci.* 179 (2) (1996) 488–508, <https://doi.org/10.1006/jcis.1996.0242>.
- [21] F. Huber, D. Schild, T. Vitova, J. Rothe, R. Kirsch, T. Schäfer, U(VI) removal kinetics in presence of synthetic magnetite nanoparticles, *Geochim. Cosmochim. Acta* 96 (2012) 154–173, <https://doi.org/10.1016/j.gca.2012.07.019>.
- [22] E. Ilton, J. Boily, E. Buck, F. Skomurski, K. Rosso, C. Cahill, J. Bargar, A. Felmy, Influence of dynamical conditions on the reduction of U(VI) at the magnetite–solution interface, *Environ. Sci. Technol.* 44 (1) (2010) 170–176, <https://doi.org/10.1021/es9014597>.
- [23] B. Kienzler, A. Loida, Endlagerrelevante Eigenschaften von hochradioaktiven Abfallprodukten. Charakterisierung und Bewertung. Empfehlung des Arbeitskreises HAW Produkte. Forschungszentrum Karlsruhe, FZKA, 2001, p. 6651.
- [24] B. Kienzler, Corrosion of canister materials for radioactive waste disposal, *Decommission. Waste Manage. ATW* 62 (8-9) (2017) 542–549.
- [25] J. Kim, B. Grambow, Geochemical assessment of actinide isolation in a German salt repository environment, *Eng. Geol.* 52 (3–4) (1999) 221–230, [https://doi.org/10.1016/S0013-7952\(99\)00007-1](https://doi.org/10.1016/S0013-7952(99)00007-1).
- [26] R. Kirsch, D. Fellhauer, M. Altmair, V. Neck, A. Rossberg, T. Fanghänel, L. Charlet, A. Scheinost, Oxidation state and local structure of plutonium reacted with magnetite, mackinawite, and chukanovite, *Environ. Sci. Technol.* 45 (17) (2011) 7267–7274, <https://doi.org/10.1021/es200645a>.
- [27] D. Latta, C. Gorski, M. Boyanov, E. O’Loughlin, K. Kemner, M. Scherer, Influence of magnetite stoichiometry on UVI reduction, *Environ. Sci. Technol.* 46 (2) (2011) 778–786, <https://doi.org/10.1021/es2024912>.
- [28] D. Li, D. Kaplan, Sorption coefficients and molecular mechanisms of Pu, U, Np, Am and Tc to Fe (hydr)oxides: a review, *J. Hazard. Mater.* 243 (2012) 1–18, <https://doi.org/10.1016/j.jhazmat.2012.09.011>.
- [29] G. Lujanienė, P. Beneš, K. Štamberg, J. Šapolaitė, D. Vopalka, E. Radžiūtė, T. Ščiglo, Effect of natural clay components on sorption of Cs, Pu and Am by the clay, *J. Radioanal. Nucl. Chem.* 286 (2) (2010) 353–359, <https://doi.org/10.1007/s10967-010-0726-y>.
- [30] J. Lützenkirchen, *Surface Complexation Modelling*, Elsevier, Burlington, 2006.
- [31] J. Mahoney, D. Langmuir, Adsorption of Sr on Kaolinite, illite and montmorillonite at high ionic strengths, *Radiochim. Acta* 54 (3) (1991) 139–144, <https://doi.org/10.1524/ract.1991.54.3.139>.
- [32] T. Missana, M. García-Gutiérrez, V. Fernández, Uranium (VI) sorption on colloidal magnetite under anoxic environment: experimental study and surface complexation modelling, *Geochim. Cosmochim. Acta* 67 (14) (2003) 2543–2550, [https://doi.org/10.1016/S0016-7037\(02\)01350-9](https://doi.org/10.1016/S0016-7037(02)01350-9).
- [33] K. Nakata, S. Nagasaki, S. Tanaka, Y. Sakamoto, T. Tanaka, H. Ogawa, Sorption and reduction of neptunium(V) on the surface of iron oxides, *Radiochim. Acta* 90 (9–11) (2002) 655–669, https://doi.org/10.1524/ract.2002.90.9-11_2002.665.
- [34] V. Neck, M. Altmair, T. Rabung, J. Lützenkirchen, T. Fanghänel, Thermodynamics of trivalent actinides and neodymium in NaCl, MgCl₂, and CaCl₂ solutions: Solubility, hydrolysis, and ternary Ca-M(III)-OH complexes, *Pure Appl. Chem.* 81 (9) (2009) 1555–1568, <https://doi.org/10.1351/PAC-CON-08-09-05>.
- [35] D.L. Parkhurst, C.A.J. Appelo, User’s guide to PHREEQC (version 2) – a computer program for speciation, batch-reaction, one-dimensional transport, and inverse geochemical calculations: U.S. Geological Survey, Water-Resour. Invest. Rep. (4259) (1999) 99, <https://doi.org/10.3133/wri994259>.
- [36] I. Pidchenko, K. Kvashnina, T. Yokosawa, N. Finck, S. Bahl, D. Schild, R. Polly, E. Bohnert, A. Rossberg, J. Göttlicher, K. Dardenne, J. Rothe, T. Schäfer, H. Geckeis, T. Vitova, Uranium redox transformations after U(VI) coprecipitation with magnetite nanoparticles, *Environ. Sci. Technol.* 51 (4) (2017) 2217–2225, <https://doi.org/10.1021/acs.est.6b04035>.
- [37] B. Powell, R. Fjeld, D. Kaplan, J. Coates, S. Serkiz, Pu(V)O₂⁺ adsorption and reduction by synthetic magnetite (Fe₃O₄), *Environ. Sci. Technol.* 38 (22) (2004) 6016–6024, <https://doi.org/10.1021/es049386u>.
- [38] B. Ravel, EXAFS analysis with FEFF and FEFFIT. Part 2: Commentary. Version 0.04, 2000.
- [39] B. Ravel, M. Newville, ATHENA, ARTEMIS, HEPHAESTUS: data analysis for X-ray absorption spectroscopy using IFEFFIT, *J. Synchrotr. Radiat.* 12 (4) (2005) 537–541, <https://doi.org/10.1107/S0909049505012719>.
- [40] I. Rojo, F. Seco, M. Rovira, J. Giménez, G. Cervantes, V. Martí, J. de Pablo, Thorium sorption onto magnetite and ferrihydrite in acidic conditions, *J. Nucl. Mater.* 385 (2) (2009) 474–478, <https://doi.org/10.1016/j.jnucmat.2008.12.014>.
- [41] J. Rothe, S. Butorin, K. Dardenne, M. Denecke, B. Kienzler, M. Löble, V. Metz, A. Seibert, M. Steppert, T. Vitova, C. Walther, H. Geckeis, The INE-Beamline for actinide science at ANKA, *Rev. Sci. Instrum.* 83 (2012), <https://doi.org/10.1063/1.3700813> 043105.
- [42] M. Rovira, S. El Amrani, L. Duro, J. Giménez, J. de Pablo, J. Bruno, Interaction of uranium with in situ anoxically generated magnetite on steel, *J. Hazard. Mater.* 147 (3) (2007) 726–731, <https://doi.org/10.1016/j.jhazmat.2007.01.067>.
- [43] A. Schnurr, R. Marsac, T. Rabung, J. Lützenkirchen, H. Geckeis, Sorption of Cm (III) and Eu(III) onto clay minerals under saline conditions: Batch adsorption, laser-fluorescence spectroscopy and modeling, *Geochim. Cosmochim. Acta* 151 (2015) 192–202, <https://doi.org/10.1016/j.gca.2014.11.011>.
- [44] T. Scott, G. Allen, P. Heard, M. Randell, Reduction of U(VI) to U(IV) on the surface of magnetite, *Geochim. Cosmochim. Acta* 69 (24) (2005) 5639–5646, <https://doi.org/10.1016/j.gca.2005.07.003>.
- [45] B. Singh, A. Jain, S. Kumar, B. Tomar, R. Tomar, V. Manchanda, S. Ramanathan, Role of magnetite and humic acid in radionuclide migration in the environment, *J. Contam. Hydrol.* 106 (3–4) (2009) 144–149, <https://doi.org/10.1016/j.jconhyd.2009.02.004>.
- [46] A. Skerencak-Frech, D. Fröhlich, J. Rothe, K. Dardenne, P. Panak, Combined time-resolved laser fluorescence spectroscopy and extended X-ray absorption fine structure spectroscopy study on the complexation of trivalent actinides with chloride at T = 25–200 °C, *Inorg. Chem.* 53 (2) (2014) 1062–1069, <https://doi.org/10.1021/ic4025603>.
- [47] E. Smailos, W. Schwarzkopf, R. Köster, Corrosion behavior of container materials for the disposal of high level waste forms in rock salt formation, INE Kernforschungszentrum Karlsruhe, 1987.
- [48] M. Usman, J. Byrne, A. Chaudhary, S. Orsetti, K. Hanna, C. Ruby, A. Kappler, S. Haderlein, Magnetite and green rust: synthesis, properties, and environmental applications of mixed-valent iron minerals, *Chem. Rev.* (2018), <https://doi.org/10.1021/acs.chemrev.7b00224>.
- [49] S. Vidojkovic, M. Rakin, Surface properties of magnetite in high temperature aqueous electrolyte solutions: a review, *Adv. Colloid Interface Sci.* 245 (2017) 108–129, <https://doi.org/10.1016/j.cis.2016.08.008>.
- [50] K. Yuan, D. Renock, R. Ewing, U. Becker, Uranium reduction on magnetite: Probing for pentavalent uranium using electrochemical methods, *Geochim. Cosmochim. Acta* 156 (2015) 194–206, <https://doi.org/10.1016/j.gca.2015.02.014>.
- [51] L. Vayssières, Thèse de doctorat, Université P. et M. Curie, Paris, 1995.
- [52] J.C. Westall, FITEQL: A Computer Program for Determination of Chemical Equilibrium Constants from Experimental Data, Version 2.0. Report 82–02, Department of Chemistry, Oregon State University, Corvallis, 1982.

Repository KITopen

Dies ist ein Postprint/begutachtetes Manuskript.

Empfohlene Zitierung:

Morelová, N.; Finck, N.; Lützenkirchen, J.; Schild, D.; Dardenne, K.; Geckeis, H.
[Sorption of americium / europium onto magnetite under saline conditions: Batch experiments, surface complexation modelling and X-ray absorption spectroscopy study](#)
2020. Journal of colloid and interface science, 561
[doi: 10.554/IR/1000104948](#)

Zitierung der Originalveröffentlichung:

Morelová, N.; Finck, N.; Lützenkirchen, J.; Schild, D.; Dardenne, K.; Geckeis, H.
[Sorption of americium / europium onto magnetite under saline conditions: Batch experiments, surface complexation modelling and X-ray absorption spectroscopy study](#)
2020. Journal of colloid and interface science, 561, 708–718.
[doi:10.1016/j.jcis.2019.11.047](#)